

Construction of a Deep-learning-based Reusability Assessment System for Large Vehicle Tires

Iori Iwata,¹ Kazuma Sakamoto,^{2*} Teruya Minakuchi,¹
Reo Ishii,² Etsuto Tashiro,³ and Yoshihiro Ueda²

¹Graduate School of Sustainable Science, Komatsu University, Komatsu, Ishikawa 923-8511, Japan

²Faculty of Product Systems Engineering and Sciences, Komatsu University, Komatsu, Ishikawa 923-8511, Japan

³Former Graduate School of Sustainable Science, Komatsu University, Komatsu, Ishikawa 923-8511, Japan

(Received December 1, 2025; accepted February 24, 2026)

Keywords: reusability assessment, object detection, YOLOv8, GPT, manufacturing date recognition

AI advancements in anomaly detection enable inspections that are more efficient and precise than human operators, enhancing recycling efficiency and supporting Sustainable Development Goals. Tire manufacturers currently rely on manual visual inspection to assess used tires for damage and manufacturing dates; however, this process suffers from skilled labor shortages and excessive time requirements. In this research, we aim to automate tire damage detection and manufacturing date recognition using deep learning on videos from standard cameras, thereby improving operational efficiency. Four experiments were conducted to validate the system. In Experiment 1, we evaluated four object detection models for damage recognition efficacy. In Experiment 2, we proposed a system for automatic reusability determination based on confidence thresholds. In Experiment 3, we utilized optical character recognition (OCR) and generative pre-trained transformer (GPT) for manufacturing date recognition, achieving 88.2% accuracy with GPT after applying image rotation and cropping. In Experiment 4, we tested an automated image cropping method, resulting in a 5.06% relative error in bounding box areas compared with manual annotation. Future work will be on combining damage and manufacturing date recognition systems and incorporating slip sign detection to further improve the classification accuracy of reusable tires.

1. Introduction

The application of AI in the field of anomaly detection has been rapidly advancing, and for some targets, it is now possible to perform inspections faster than can be done by human operators. In addition, while detection using dedicated sensors has been widely employed, recent approaches increasingly rely on not only sensors but also video cameras, leveraging object detection algorithms for visual-based detection. In tire-related machinery manufacturing, used tires are reusable, and at present, workers visually inspect surface damage and manufacturing date codes to classify tires according to whether they can be reused. However, this process faces

*Corresponding author: e-mail: kazuma.sakamoto@komatsu-u.ac.jp
<https://doi.org/10.18494/SAM6089>

challenges such as a shortage of personnel with the required inspection skills and the long time required for manual inspection. Motivated by this background, research on AI-based anomaly detection has been actively conducted in this field as well. Tatsumoto and Araki developed an automatic defect detection system for metal press parts using you only look once v5 (YOLOv5), reporting a detection accuracy of 99%.^(1,2) Arima *et al.* and Redmon and Farhadi achieved an accuracy of 82% in defect detection for industrial products using YOLOv2.^(3,4) Furthermore, Nakajima *et al.* and Girshick *et al.* demonstrated a detection accuracy of 81% for plastic product appearance inspection using region-based convolutional neural network (R-CNN),^(5,6) and Takagi *et al.* and Dosovitskiy *et al.* reported high accuracy in detecting defects in forged parts using Vision Transformer.^(7,8) As such, research on appearance inspection and defect detection using object detection models has been progressing for a wide range of industrial products. Most existing research, however, focuses on products where all nondefective items share an identical shape, and the task is to distinguish these from defective items that contain local anomalies. There is little research on target products whose shapes vary even among nondefective items, which is the topics of our work herein. In the case of reused tires, even nondefective ones exhibit diverse characteristics, such as differences in the remaining tread pattern and the degree of rubber wear.

Here, we present research focusing on tires and similar objects. Saleh *et al.* compared nine transfer learning models on X-ray images, finding that Xception achieved the highest accuracy. However, their research was limited to binary classification and struggles with data imbalance and detecting minute defects.⁽⁹⁾ Kuric *et al.* and Simonyan and Zisserman developed a hybrid 2D/3D system using unsupervised learning and VGG-16 for sidewall inspection, but they faced challenges regarding the computational cost of clustering algorithms and restricted their analysis to the sidewall.^(10,11) Lin achieved 94.7% accuracy in detecting tire cracks using an improved ShuffleNet architecture, although the research's focus on cracks alone and reliance on a small dataset limit the model's generalization.⁽¹²⁾ Mignot *et al.* proposed a two-stage multimodal approach to inspect all tire zones for defects and severity, but they encountered significant latency issues with 20 s inference times and difficulties in annotating diffused defects.⁽¹³⁾

To address these challenges, in this research, we propose a novel method for assessing tire reusability by integrating a YOLOv8 object detection model with a generative pre-trained transformer (GPT) manufacturing-date recognition technique.^(14,15) By combining the two models, the proposed system first automatically extracts the manufacturing date printed on the tire, determines reusability on the basis of the manufacturing date, and then detects surface damage to make a final reusability decision. In this paper, we validate each component separately; integration is future work. Although the proposed approach still has limitations in real-time processing performance and recognition accuracy compared with prior research, the integration of deep learning and large language models suggests the potential to build systems that are more efficient and accurate than conventional methods. In particular, at present, a large number of tires must be processed each day, and the workflow has not yet been sufficiently streamlined. In this study, we focus on identifying clearly non-reusable tires in the stage prior to the final detailed visual inspection.

2. Methods

This research is divided into four experiments. Experiments 1 and 2 involve classification based on damage detection, whereas Experiments 3 and 4 involve classification based on manufacturing date.

2.1 Experiment 1 method

Figure 1 illustrates the processing flow of Experiment 1. In this experiment, we evaluated the tire damage detection performance of four object detection models. The input data are tire-damage images, as shown in Fig. 2. The object detection models used are Faster R-CNN, YOLOX, YOLOv8, and SSD.^(14,16–18)

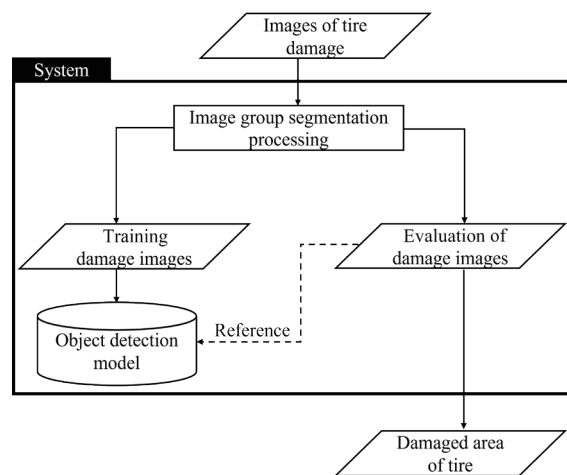


Fig. 1. Experiment 1 flow.



Fig. 2. (Color online) Example of input image.

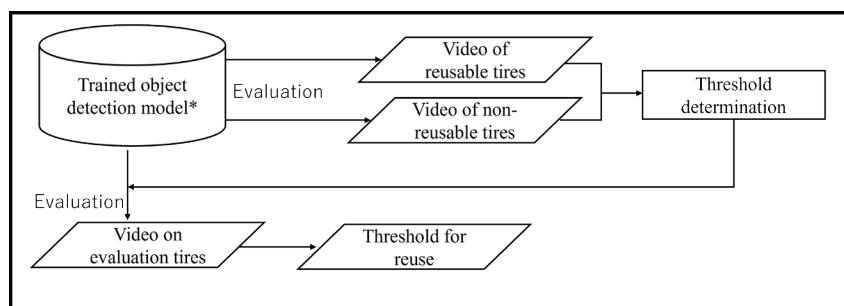
The imaging environment used in this experiment is described below. As shown in Fig. 2, images were captured so that the damaged region on the front side of the tire was visible. The tire was rotated as necessary so that the damage remained within the camera's field of view. The acquired images were randomly divided into training and test datasets at a ratio of 8:2. For the training data, three of the authors annotated the regions they judged to be damaged by assigning labels, and these annotations were used to train each object detection model. In this research, damage was defined as visually identifiable surface anomalies in RGB images, including cracks, chips, and wear that may affect tire reusability. Here, "wear" mainly refers to abnormal wear patterns (e.g., uneven or stepped wear), while uniform normal wear was not regarded as damage. Artifacts such as dirt, shadows, specular reflections, manufacturing marks, and motion blur were excluded. The trained models were then evaluated on the test data to assess how accurately they could detect tire damage.

As evaluation metrics, we used recall, precision, and F1-score. Recall represents the proportion of truly damaged regions that were correctly detected as damaged. Precision represents the proportion of regions predicted as damaged that were actually damaged. The F1-score is the harmonic mean of recall and precision and serves as an indicator that jointly evaluates both metrics. Given the critical importance of damage in our setting, we place particular emphasis on recall.

2.2 Experiment 2 method

The system flow for this experiment is illustrated in Fig. 3. Input videos were captured from the front of a rotating tire, and inference was performed using the object detection model trained in Experiment 1. On the basis of inference results, we determined thresholds to classify tires as reusable or non-reusable. Owing to the limited dataset size, we employed the leave-one-out cross-validation (LOOCV) method.

Imaging Conditions: As shown in Fig. 4, the camera was positioned to capture more than half of the tire's front surface. Videos were recorded while rotating the tire at 6 rpm. Data corresponding to one full revolution was extracted for analysis; at a frame rate of 30 fps, this corresponds to 300 frames per tire.



* Same as model experiment 1

Fig. 3. Experiment 2 flow.



Fig. 4. (Color online) Example of image.

Threshold Determination: We established thresholds for the reusability decision using the model trained in Experiment 1. We analyzed inference results for both reusable and non-reusable tires by aggregating the number of detected defects at varying confidence scores. The confidence score yielding an average of one detection per tire was defined as the “boundary” for each class. We defined two specific thresholds (see Fig. 5).

Threshold (a): This is the midpoint between the boundaries of the reusable and non-reusable classes.

Threshold (b): To strictly minimize the risk of passing non-reusable tires, we set Threshold equal to the boundary value of the reusable class.

Evaluation: In the LOOCV procedure, one sample was used for evaluation while the remaining samples constituted the training set (used here to determine the thresholds). This process was repeated until every sample had been evaluated. A tire was classified as non-reusable if at least one defect was detected during the evaluation. The final performance was calculated by averaging the results across all iterations.

2.3 Experiment 3 method

In this experiment, we evaluate how accurately the manufacturing date of a tire can be recognized using an optical character recognition (OCR) tool. In addition, we conduct a recognition experiment using the API of GPT, a large language model. To investigate the effects of rotation and background, we then rotate the images so that the characters appear upright, crop the regions containing the manufacturing date, and perform the same experiments on these cropped images. The input images are tire images that include the manufacturing date, as shown in Fig. 6. The OCR tool used in this experiment is Tesseract, and the GPT model used is GPT-4o.^(19,20)

The manufacturing date of a tire is engraved as shown in Fig. 6. It may be recessed, as in Fig. 6(a), or embossed, as in Fig. 6(b). The last four digits represent the manufacturing date, where the last two digits indicate the year of manufacture and the first two digits indicate the week number within that year. Therefore, the tire in Fig. 6(a) was manufactured in the 3rd week of 2017, and the tire in Fig. 6(b) was manufactured in the 29th week of 2021.

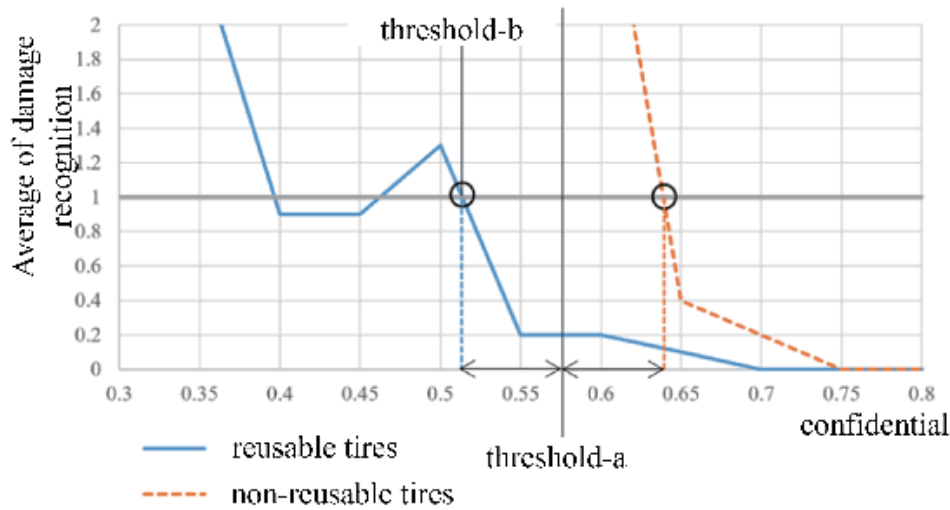


Fig. 5. (Color online) Example of average damage recognition count graph.

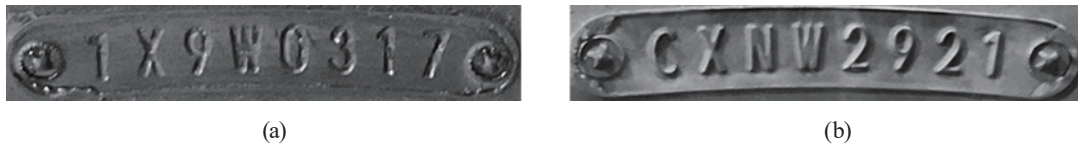


Fig. 6. Examples of tire manufacturing date. (a) Manufacturing date stamped on the tire. (b) Manufacturing date embossed on the tire.

The imaging environment used in this experiment is described below. Two types of tire were used as targets: those from passenger cars and those from large vehicles. For passenger cars, images were captured so that the manufacturing date was visible, as shown in Fig. 7(a). For large vehicles, the sidewall of the tire was photographed so that the manufacturing date on the side surface was visible, as shown in Fig. 7(b).

In addition, the usage of OCR and GPT in this experiment is described below. Using OCR, which is a character recognition technology, we input tire images that include the manufacturing date and obtain the characters contained in the images as output. The processing flow when using GPT is shown in Fig. 8. First, an image containing the manufacturing date is converted into base64 format, which can be fed into GPT. Then, a prompt is designed to obtain better recognition results, and the base64-encoded image together with the prompt is given as input.

Moreover, since the acquired images capture the entire tire, we investigate the influence of rotation and background by rotating and cropping the images so that only the region containing the manufacturing date remains. For the evaluation, we regard a case as correct when the manufacturing date output by the OCR tool or GPT exactly matches the true manufacturing date, and we compute the accuracy as the ratio of correct cases.

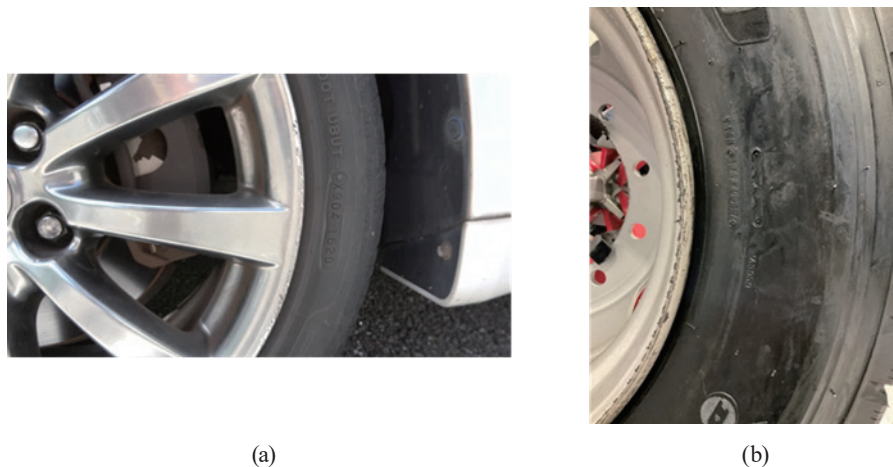


Fig. 7. (Color online) Examples of images showing the manufacturing date. (a) Manufacturing date of passenger car tires. (b) Manufacturing date of large-vehicle tires.

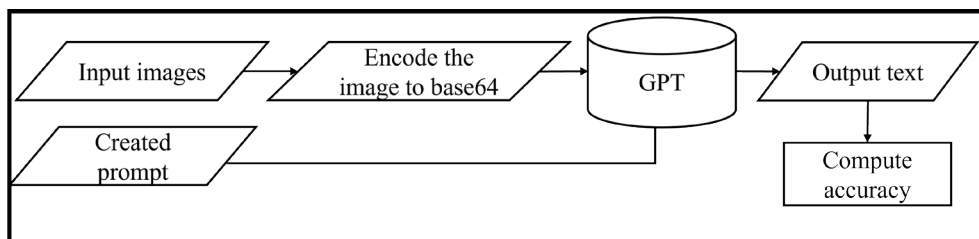


Fig. 8. Flow of GPT-based manufacturing date recognition.

2.4 Experiment 4 method

The processing flow of Experiment 4 is shown in Fig. 9. The purpose of this experiment is to automate the cropping process that was performed manually in Experiment 3. The input is a rotating tire video in which the manufacturing date of the tire appears. An object detection model is applied to this video to recognize the characteristic shape of the region where the manufacturing date is engraved, as shown in Fig. 10, and to extract the corresponding bounding-box region. The number of pixels in the extracted region is then compared with that of the annotated region created manually, and this comparison is used for evaluation. In this experiment, YOLOv8 is adopted as the object detection model.

The image acquisition in this experiment was conducted in the same manner as in Experiment 3. All images used in Experiment 3 were annotated and used as training data to train the object detection model. The evaluation videos were then split into individual frames, which were used as test data for evaluation.

For pixel-count computation, the bounding-box regions output by the object detection model were extracted as images, and the number of pixels in these images was calculated. Likewise, for the ground-truth data obtained by manual annotation, the number of pixels in the annotated

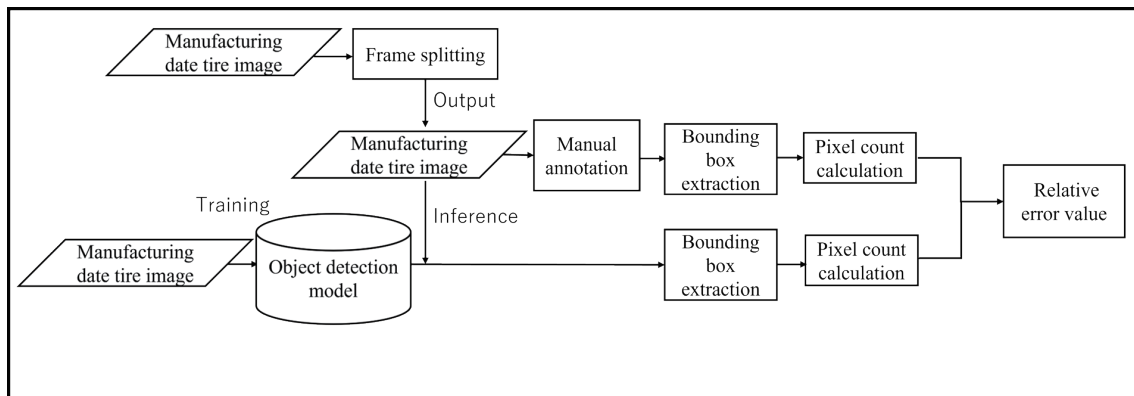


Fig. 9. Flow of Experiment 4.



Fig. 10. Distinctive shape of the manufacturing date stamp.

regions was calculated. The evaluation was performed by computing the relative error between the number of pixels in the model-output regions and that in the manually annotated regions and using this relative error as the evaluation metric.

3. Experimental Data and Result

This research is broadly divided into two parts, as shown in Fig. 11. The first part consists of Experiments 1 and 2, which focus on the development of a classification system for tire damage detection. In Experiment 1, we evaluated the ability of four object detection models to recognize tire damage. In the following Experiment 2, we investigated a method for determining whether a tire is reusable using the object detection model trained in Experiment 1.

The second part, consisting of Experiments 3 and 4, addresses the development of a classification system for manufacturing date recognition. In Experiment 3, we perform experiments on the recognition of manufacturing dates using OCR tools and GPT, as well as examining the effects of image rotation and cropping on recognition accuracy. In Experiment 4, we built an automatic method for performing the cropping process that was validated in Experiment 3 and evaluated its effectiveness.

3.1 Experiment 1 (Damage detection using object detection models)

The damage images used for training the object detection model were captured using an iPad Air (4th generation). A total of 81 images of the damaged areas were captured, and data augmentation was applied by flipping the images vertically, horizontally, and both vertically and horizontally. As a result, 267 training images and 67 test images were obtained. The imaging

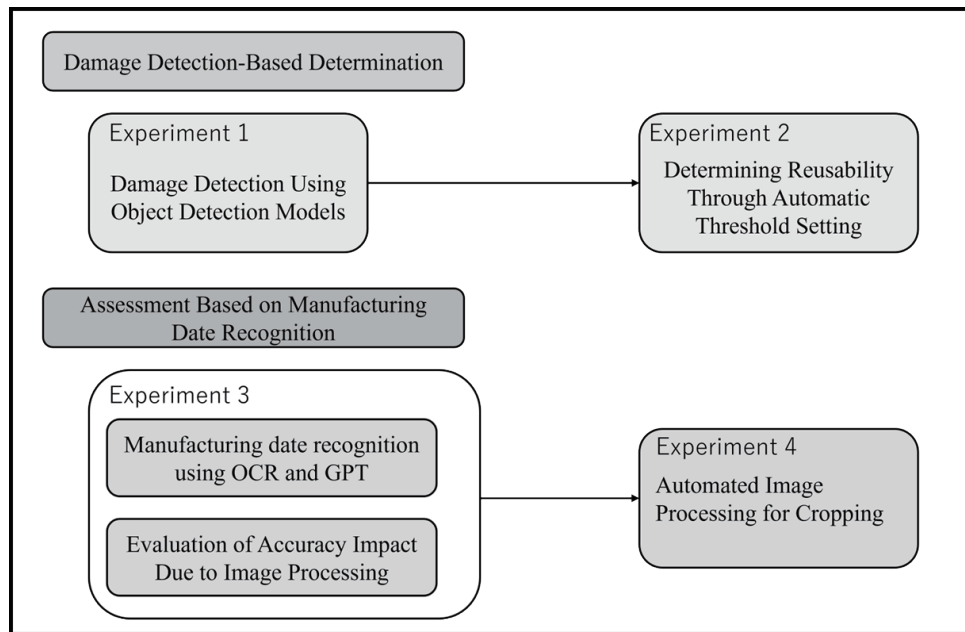


Fig. 11. Overview of this research.

method for this research involved adjusting the field of view to ensure that the tire damage was within the frame. No specific settings for distance or orientation were applied in order to improve the generalization ability of the model.

For evaluation in this research, we calculate recall, precision, and F1-score by comparing the bounding boxes output by the object detection models with the manually annotated ground-truth bounding boxes. Additionally, the inference time for each model is measured. Examples of bounding box outputs for Faster R-CNN, SSD, YOLOX, and YOLOv8 are shown in Fig. 12. The recall, precision, and F1-score for each model are summarized in a table.

Failure cases included misclassifying tire grooves as damage or missing small damages. This could be due to the presence of many differently shaped and sized damages in the evaluation data that were not represented in the training data. Therefore, to improve accuracy, increasing the variety of damage in the training data and applying image augmentation techniques, such as scaling down images, to create data for smaller damages not included in the training set could be considered.

The recall, precision, and F1-score for each object detection model are shown in Table 1. From Table 1, it can be seen that Faster R-CNN achieved relatively high precision, recall, and F1-score. However, its inference time was the longest among the models used in this experiment, taking approximately 2 s. SSD, YOLOX, and YOLOv8 were able to perform inference in just a few milliseconds, but none of these models showed high accuracy across all metrics. Among the models capable of real-time inference, YOLOv8 produced the best results, so YOLOv8 will be used for subsequent experiments.

In our experimental setting, the inference speed of Faster R-CNN is sufficient for practical use. However, from the perspective of future deployment, a certain level of accuracy is required,

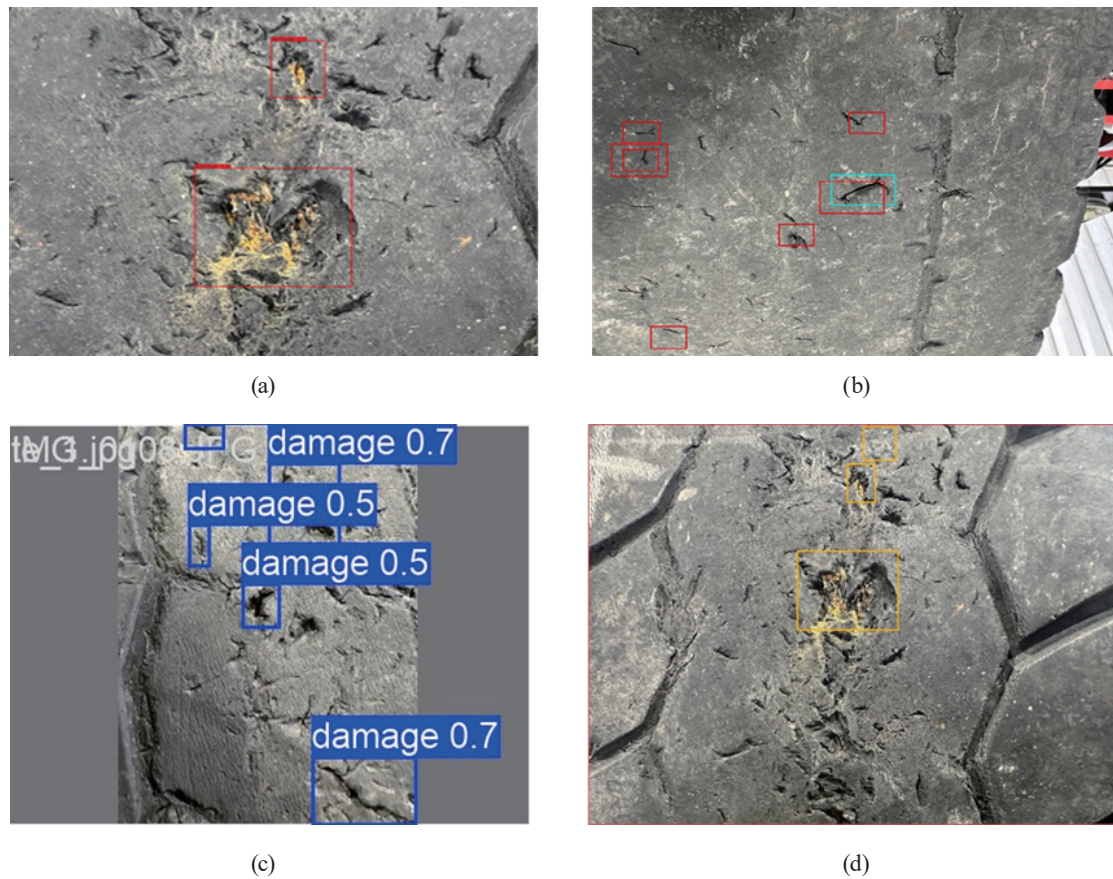


Fig. 12. (Color online) Examples of detection results by each object detection model. (a) Faster R-CNN, (b) SSD, (c) YOLOv8, (d) YOLOX.

Table 1
Accuracy of each object detection model.

	Recall (%)	Precision (%)	F1-score (%)
Faster R-CNN	68.7	80.7	74.2
YOLOv8	48.1	52.6	50.3
YOLOX	37.3	71.4	49.0
SSD	21.9	27.7	24.5

while faster processing would directly contribute to higher productivity. Therefore, we plan to continue investigating performance improvements and select the most appropriate model by balancing accuracy and computational efficiency. In comparing YOLOX and YOLOv8, minimizing missed detections of damage is critical in our application; therefore, recall is the most important evaluation metric in this study. For this reason, we consider YOLOv8 to be more suitable for our purpose. In Experiment 2, the model trained in Experiment 1 will be used to propose a method for defect detection using an object detection model that does not achieve high accuracy for damage detection.

3.2 Experiment 2 (Determining reusability through automatic threshold setting)

In this experiment, we perform a classification of reusable tires using an object detection model that did not achieve high accuracy in damage detection. The threshold setting and evaluation videos were obtained by rotating the tire at a speed of 6 rpm, with the video camera fixed to capture the front of the tire within the field of view. A video of one full tire rotation (approximately 300 frames) was recorded. A total of 10 reusable tires and 10 non-reusable tires were recorded. The object detection model used was YOLOv8, which was confirmed to allow for fast inference in Experiment 1.

The inference results for the 10 reusable and 10 non-reusable tires are shown in Fig. 13. The horizontal axis represents the confidence level of data predicted as damage, whereas the vertical axis represents the average number of detections per tire at each confidence level. As shown in Fig. 13, by identifying the confidence level at which the average number of detections per tire is 1, we can determine the boundaries for reusable and non-reusable tires and calculate system thresholds a and b. The classification results of the evaluation videos using the Leave One Out method are shown in Tables 2 and 3. With threshold a, the overall accuracy was 65.0%, the accuracy for reusable tires was 80.0%, and the accuracy for non-reusable tires was 50.0%. With threshold b, the overall accuracy increased to 75.0%, the accuracy for reusable tires was 70.0%, and the accuracy for non-reusable tires was 80.0%.

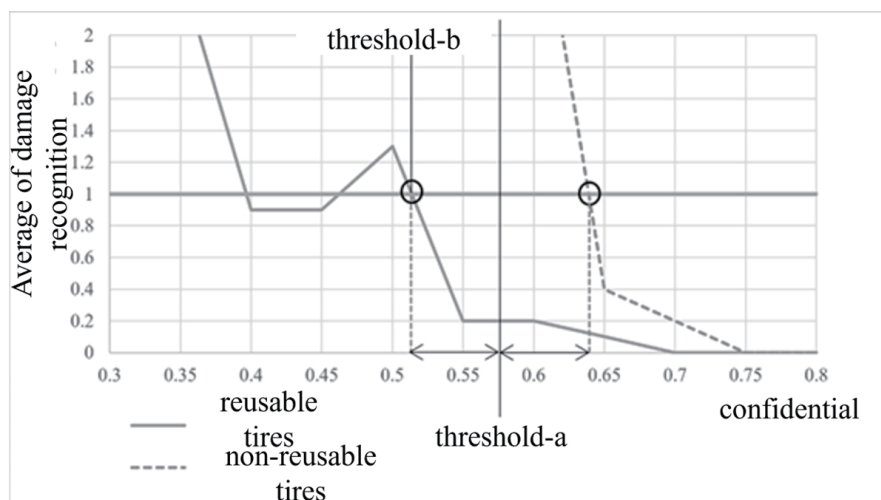


Fig. 13. Average number of damage detections.

Table 2
Classification results using threshold a.

	Accuracy (%)
Non-reusable tire	50.0
Reusable tire	80.0
Average	65.0

Table 3
Classification results using threshold b.

	Accuracy (%)
Non-reusable tire	80.0
Reusable tire	70.0
Average	75.0

The cause of these results can be attributed to missed damage detection and high confidence bounding boxes being output for areas of reusable tires that did not have visible damage. This issue depends on the accuracy of the object detection model, and we believe it can be resolved by using a better model.

Additionally, to maximize safety, it is crucial to correctly identify non-reusable tires with 100% accuracy. However, it was not possible to automatically set a threshold for this within the current method, and this will be a subject for future improvement.

3.3 Experiment 3 (Assessment based on manufacturing date recognition)

In this experiment, we use OCR tools and the large language model GPT to evaluate the recognition of manufacturing dates. The images containing the manufacturing dates were captured using an iPad Air (4th generation). A total of 71 images from passenger cars and 17 images from large vehicles were acquired.

The OCR tool used was Tesseract, and the GPT model was GPT-4o. In addition, the prompt for the GPT API was designed to extract the manufacturing date from the image and output it in a format that facilitates subsequent processing. In the experiment using a passenger car, we set the user rule: “When was this tire manufactured? Please write in ANS=” with numbers and avoid using month names in your response.” For the experiment with large vehicles, the system rule was set as “You are an Optical Character Recognition (OCR) machine. You will extract all the characters from the image file provided by the user, and you will only provide the extracted text in your response. As an OCR machine, you can only respond with the extracted text. The response should be output in JSON format.” and the user rule was set as “What year was this tire manufactured?” In our experimental setting, the prompts differ between passenger cars and large vehicles; therefore, we do not perform a direct comparison between the two. The evaluation method involves comparing the extracted manufacturing date with the actual manufacturing date. If they match exactly, the result is considered correct.

Furthermore, as shown in Fig. 14, to examine the impact of rotation and background on the accuracy, the images were rotated so that the manufacturing date appeared upright, and the area



Fig. 14. Example of images before and after image processing. (a) Example of unprocessed image. (b) Example of processed image after rotation and cropping.

outside the manufacturing date was cropped. Similar experiments were conducted on these processed images.

The recognition results using Tesseract are shown in Table 4. The OCR tool failed to recognize the manufacturing date at all. This is because the OCR tool used in this experiment is primarily designed for images with black text on white paper, and it is not intended for use with images where text is engraved or embossed on black materials, as in the conditions of this experiment. Therefore, it is believed that if the image can be binarized by utilizing the subtle pixel value differences between the material and the text and processed so that the text appears in black on a white background, recognition would be possible.

The results of GPT and the recognition results after image processing are shown in Table 5. The accuracy before image processing was 23.5%, whereas the accuracy after rotation and cropping was 88.2%. This demonstrates that image processing through rotation and cropping significantly improves the recognition accuracy of manufacturing dates.

The low accuracy before processing can be attributed to the fact that GPT, a large language model, has been trained on text available on the internet, which is typically in a human-readable orientation and size, with clearly displayed characters. Consequently, it has not been trained on other types of character, such as those with rotated orientations or with extensive background information. Therefore, we believe that adding additional training for GPT on such characters can improve its recognition ability.

3.4 Experiment 4 (Automated image processing for cropping)

This experiment focuses on automating the cropping of the manufacturing date section from tire videos that contain the manufacturing date. Using an object detection model, we detect the characteristic shape of the region where the manufacturing date is engraved and perform cropping by extracting the bounding box of that region as a single image. The evaluation is performed by calculating the relative error between the pixel count of the bounding box image output by the object detection model and the pixel count of the manually annotated region.

The tire was rotated at a speed of 6 rpm, and videos were captured from an angle that displayed the sidewall of the tire, ensuring that the manufacturing date was visible. A total of 10 videos, each about 20 frames long, were obtained using a 30 fps video camera. The object detection model used in this experiment was YOLOv8, which was confirmed to enable fast inference in Experiment 1.

Table 4
Manufacturing date recognition results using OCR tools.

Target	Accuracy rate after image processing (%)
Large vehicles	0.00

Table 5
Manufacturing date recognition results using GPT.

Target	Accuracy rate before image processing (%)	Accuracy rate after image processing (%)
Passenger cars	25.4	70.4
Large vehicles	23.5	88.2

Examples of the extracted images using the object detection model and the manually annotated manufacturing date sections are shown in Figs. 15 and 16. As seen in these figures, the object detection model was able to output the same regions as those manually annotated. Additionally, out of the 10 tire videos, cropping was successful for 8 videos, as shown in Table 6. The reason for the failure to trim certain videos was likely due to the unclear appearance of the manufacturing date, as shown in Fig. 17. In such cases, since the tire is likely to be highly worn and non-reusable, we classify it as non-reusable.

For the 125 frames that the object detection model was able to recognize, the total pixel count of the images extracted by the model and the manually annotated manufacturing date sections are shown in Table 7. From Table 7, the total pixel count of the images extracted by the object detection model was 7315577 pixels, whereas the total pixel count of the manually annotated manufacturing date section for the same frames was 6963376 pixels. Therefore, the relative error was 5.06%, indicating that a high level of accuracy was achieved.



Fig. 15. (Color online) Example of manual annotation.



Fig. 16. (Color online) Object-detection-model-based extracted images.

Table 6
Percentage of manufacturing date fields successfully extracted.

	Ratio (%)
10 Tire Videos	80.0



Fig. 17. (Color online) Example of image where the distinctive mark was unclear.

Table 7
Results of comparing manual verification and automated methods.

Total pixels annotated manually	Total pixels in extracted images using object detection models	Relative error (%)
6963376	7315577	5.06

3.5 Considerations on the four experiments

In this research, we conducted four experiments to develop a system capable of assessing tire reusability. In Experiment 1, we searched for an object detection model suitable for our setting, and in Experiment 2, we determined an appropriate decision threshold to classify tires using the selected model. As shown in Experiment 2, threshold tuning improved classification performance and suggested high accuracy in determining reusability. The results of these two experiments showed that the current model achieves an accuracy of approximately 80%; however, further improvements are expected by exploring alternative models. In addition, Experiments 3 and 4 suggest that tire reusability can be inferred from the manufacturing date imprinted on the tire.

These experiments resulted in a system that achieved an accuracy of approximately 80% in assessing tire reusability. This suggests the system's potential feasibility for deployment in real-world operating environments. In future work, we plan to integrate these two components into a two-stage framework: the system will first screen tires on the basis of manufacturing date and then perform damage detection only for tires deemed reusable. We will therefore implement the integrated model and conduct a comprehensive evaluation in subsequent work. This approach is expected to improve overall performance compared with a damage-only reusability assessment.

4. Conclusions

In this research, we focused on the defect classification of products using object detection models. Specifically, the research addressed the classification of defective products when anomalies with low detection accuracy are present in object detection models. In Experiment 1, we evaluated the ability of four object detection models—Faster R-CNN, SSD, YOLOX, and YOLOv8—to recognize tire damage. The highest accuracy was achieved by Faster R-CNN, with a recall of 68.7% and a precision of 80.7%. However, the inference time was long, which made the results unsuitable for the current purpose. For models capable of real-time recognition, both recall and precision were not sufficiently high, indicating that improvements are needed for classifying reusable tires.

In Experiment 2, we proposed a method to automatically set the threshold for recognizing damage using YOLOv8, which showed relatively good accuracy and was capable of real-time recognition. The accuracy for non-reusable tires was 80.0%, whereas that for reusable tires was 70.0%. Further improvement in accuracy is needed, which may require the enhancement of the damage recognition performance in Experiment 1 and developing better threshold-setting methods.

In Experiment 3, we used the GPT API to recognize manufacturing dates on images that had been processed, achieving a high accuracy of 88.2%. We confirmed that image processing

techniques such as rotation and cropping significantly improve recognition accuracy. To further enhance the accuracy, exploring better prompts and fine-tuning the large language model, which was not feasible in this research owing to cost constraints, would be effective.

In Experiment 4, we proposed and experimented with an automated image processing method for cropping, which was confirmed to be effective in Experiment 3. The cropping success rate was 80.0%, and the relative error in the pixel count of the cropped images was 5.06%, indicating an accuracy comparable to manual processing.

We plan to integrate the two models into a two-stage framework and build a unified classification system to further improve performance, while also investigating how to demonstrate its practical utility under real-world operating conditions.

In the future, research will focus on slip signs, which, like damage and manufacturing dates, are also critical for determining tire reusability. While slip signs are an important factor in this decision-making process, the single-view image recognition AI used in this research was unable to capture the degree of tire wear. For recognizing slip signs, we believe noncontact distance sensors, such as ultrasonic or infrared sensors, may be effective.

Acknowledgments

We are deeply grateful to ONODANI Co., Ltd. for providing the data and for their helpful advice throughout this project.

References

- 1 Y. Tatsumoto and R. Araki: Proc. Kyushu Branch Inst. Electron. Inf. Commun. Eng. (2023) 439.
- 2 Ultralytics, <https://docs.ultralytics.com/ja/models/yolov5/> (accessed April 2025).
- 3 K. Arima, F. Nagata, T. Shimizu, H. Kato, and K. Watanabe: Proc. 2022 Annu. Conf. Soc. Ind. Appl. Eng. (2022) 43.
- 4 J. Redmon and A. Farhadi: Proc. 2017 IEEE Conf. Computer Vision and Pattern Recognition (CVPR) (2017) 7263. <https://doi.org/10.1109/CVPR.2017.690>
- 5 A. Nakajima, K. Nishitani, K. Motegi, Y. Tanaka, and Y. Shiraishi: J. Electron. Packag. Soc. **22** (2019) 559.
- 6 R. Girshick, J. Donahue, T. Darrell, and J. Malik: Proc. 2014 IEEE Conf. Computer Vision and Pattern Recognition (CVPR) (2014) 580. <https://doi.org/10.1109/CVPR.2014.81>
- 7 Y. Takagi, K. Fujita, M. Nakagawa, and T. Yosetsu: 2023 Forum Inf. Sci. Technol. (FIT) (2023) 189.
- 8 A. Dosovitskiy, L. Beyer, A. Kolesnikov, D. Weissenborn, X. Zhai, T. Unterthiner, M. Dehghani, M. Minderer, G. Heigold, S. Gelly, J. Uszkoreit, and N. Houlsby: Proc. Int. Conf. Learning Representations (ICLR) (2021). <https://openreview.net/forum?id=YicbFdNTTy>
- 9 R. A. A. Saleh, M. Z. Konyar, K. Kaplan, and H. M. Ertunç: Neural Comput. Appl. **36** (2024) 12483. <https://doi.org/10.1007/s00521-024-09664-4>
- 10 I. Kuric, J. Klarák, M. Sága, M. Cisar, A. Hajdučík, and D. Wiecek: Sensors **21** (2021) 7073. <https://doi.org/10.3390/s21217073>
- 11 K. Simonyan and A. Zisserman: Proc. 3rd Int. Conf. Learning Representations (ICLR) (2015) 1. <https://arxiv.org/abs/1409.1556>
- 12 S.-L. Lin: Sci. Rep. **13** (2023) 8027. <https://doi.org/10.1038/s41598-023-35227-z>
- 13 T. Mignot, F. Ponchon, A. Derville, S. Duffner, and C. Garcia: J. Intell. Manuf. **36** (2025) 3427. <https://doi.org/10.1007/s10845-024-02378-3>
- 14 Ultralytics: <https://docs.ultralytics.com/ja/models/yolov8/> (accessed January 2025).
- 15 A. Radford, K. Narasimhan, T. Salimans, and I. Sutskever: https://cdn.openai.com/research-covers/language-unsupervised/language_understanding_paper.pdf (2018).
- 16 R. Girshick: Proc. 2015 IEEE Int. Conf. Computer Vision (ICCV) (2015) 1440. <https://doi.org/10.1109/ICCV.2015.169>

- 17 Z. Ge, S. Liu, F. Wang, Z. Li, and J. Sun: arXiv:2107.08430 (2021). <https://arxiv.org/abs/2107.08430>
- 18 W. Liu, D. Anguelov, D. Erhan, C. Szegedy, S. Reed, C.-Y. Fu, and A. C. Berg: Computer Vision – ECCV 2016 (2016) 21. https://doi.org/10.1007/978-3-319-46448-0_2
- 19 A. Karpathy, G. Toderici, S. Shetty, T. Leung, R. Sukthankar, and L. Fei-Fei: Proc. 2014 IEEE Conf. Computer Vision and Pattern Recognition (CVPR) (2014) 1725. <https://doi.org/10.1109/CVPR.2014.223>
- 20 OpenAI: arXiv:2303.08774 (2023). <https://arxiv.org/abs/2303.08774>

About the Authors



Iori Iwata received his M.S. degree from the Graduate School of Sustainable Systems Science, Komatsu University, Japan, in 2024, where he is currently pursuing his Ph.D. degree. His research interests include image recognition, tactical analysis, and sports informatics.



Kazuma Sakamoto received his B.S., M.S., and Ph.D. degrees in informatics from Kansai University, Japan, in 2015, 2018, and 2021, respectively. Since 2021, he has been an assistant professor at the Faculty of Production Systems Engineering and Sciences, Komatsu University, Japan. His research interests include web mining, natural language processing, image processing, and sports informatics. (kazuma.sakamoto@komatsu-u.ac.jp)



Teruya Minakuchi received his B.S. degree in production systems engineering and sciences from Komatsu University, Japan, in 2025, where he is currently pursuing his M.S. degree at the Graduate School of Sustainable Systems Science. His research interests include web mining and natural language processing.



Reo Ishii is currently pursuing his bachelor's degree at Komatsu University, Japan. His research interests include computer vision and pattern recognition.



Etsuto Tashiro received his B.S. degree in production systems engineering and sciences from Komatsu University, Japan, in 2023, where he also received his M.S. degree from the Graduate School of Sustainable Systems Science in 2025.



Yoshihiro Ueda received his Ph.D. degree in mathematical information science from Kanazawa University, Japan, in 2001. Since 2021, he has been a professor at the Faculty of Production Systems Engineering and Sciences, Komatsu University, Japan. His research interests include productivity improvement, labor saving, automation using data science, and human centric system development. (yoshihiro.ueda@komatsu-u.ac.jp)